

# Structural studies of $(\text{Ru}_{0.84}\text{Zr}_{0.16})_{1-x}\text{B}_x$ metallic glasses with $0.46 \leq x \leq 0.52$

Madhav Mehra, Arthur Williams, and William L. Johnson

*W. M. Keck Laboratories for Engineering Materials, California Institute of Technology, Pasadena, California 91125*

(Received 5 November 1982; revised manuscript received 10 February 1983)

In this paper we present detailed x-ray-diffraction studies on the metallic glass system  $(\text{Ru}_{0.84}\text{Zr}_{0.16})_{1-x}\text{B}_x$  over the composition range  $0.46 \leq x \leq 0.52$ . Available, binary dense-random-packing models are not successful in explaining the structure of these glasses. The presence of a peak in the  $G(r)$  at a distance of  $\sqrt{2}$  times the nearest-neighbor separation has led us to invoke the packing of trigonal prisms to explain their structure. With this proposed short-range order, we find that we can reproduce the main features of the experimentally obtained reduced radial distribution functions. These glasses have very high atomic densities and are found to be extremely brittle.

## INTRODUCTION

In a recent publication,<sup>1</sup> the authors reported the work done on a ternary, rhodium-based, metallic glass system. While the metalloid content of most "traditional" transition-metal-metalloid glasses ranges approximately between 17 and 25 at. %, these alloys with a nominal composition of  $\text{Rh}_{0.92-x}\text{B}_x\text{Si}_{0.08}$  had a total metalloid content of up to 40 at. %. Some work on Ni-B and Co-B metallic glasses with B contents as high as 40 at. % have also been reported.<sup>2,3</sup> Limitations to the formation of an amorphous phase in the "traditional" transition-metal-metalloid alloys to the above-mentioned composition range have been interpreted in terms of models where the metalloid atoms occupy the larger polyhedral holes inherent in an amorphous structure of dense random packing (DRP) of metal atoms.<sup>4</sup> The number fraction of these holes is about 20%. No existing models have been used, however, to explain the formation of amorphous alloys with a much higher metalloid content. We report here on the discovery of some ruthenium-based, ternary metallic glasses with boron concentrations between 36 and 54 at. %. X-ray-diffraction studies are presented along with the density data. The observed reduced radial distribution functions are explained in terms of ideas proposed by Gaskell.<sup>5</sup>

Certain similarities between these and the glasses in the Rh-B-Si series do exist, especially in the reduced radial distribution functions, but physical properties differ substantially. The ruthenium-based glasses are extremely brittle in contrast to the ductile foils formed by the rhodium glasses. They are also easily attacked chemically, unlike the rhodium glasses.

## EXPERIMENTAL PROCEDURES

The alloys were prepared by rf-induction-melting the accurately weighed constituents on a silver boat in an argon atmosphere. The ingots were broken and remelted to ensure a homogeneous composition. Amorphous samples were then prepared by rapidly quenching the melt in a helium atmosphere using the "piston-and-anvil" technique.<sup>6</sup> The foils produced were typically 40  $\mu\text{m}$  thick and 1.5 cm diam. Owing to the extreme brittleness of the samples, however, some quenches resulted in fragments. In fact, there was a very good correspondence between a good quench and obtaining a whole, unbroken foil. Sam-

ples were checked for the absence of crystallinity using a Norelco scanning diffractometer and  $\text{Cu K}\alpha$  radiation. Detailed diffraction studies were performed in the transmission geometry using  $\text{Mo K}\alpha$  radiation (0.7107 Å) on a General Electric XRD-5 diffractometer. A focusing LiF monochromator was placed in the diffracted beam to help eliminate Compton scattering and elastic scattering from photons with energies other than  $\text{Mo K}\alpha$ . The data obtained were corrected for background, polarization, absorption, and Compton scattering and were then normalized using the "high-angle method."<sup>7</sup> The data acquisition was carried out in a constant count mode with  $10^4$  counts at each data point, restricting the statistical errors to within  $\pm 1$  %.

The density measurements were made on whole foils using the hydrostatic weighing technique with toluene as a working fluid. The absolute errors in the density were  $\pm 0.5$  %.

## RESULTS AND ANALYSIS

The ternary alloy  $(\text{Ru}_{0.84}\text{Zr}_{0.16})_{1-x}\text{B}_x$  could be made amorphous when quenched from the melt over the composition range  $0.36 \leq x \leq 0.54$ . The concentration of zirconium in these alloys was found to be extremely critical, and amorphous foils could be obtained only with zirconium concentrations ranging between 6 and 10 at. %. Attempts to substitute titanium for zirconium were unsuccessful, although we were able to quench  $\text{Pt}_{47}\text{Zr}_9\text{B}_{44}$  into the glassy state.

The diffraction patterns for these materials exhibit extremely broad maxima. Figure 1 shows the diffraction pattern for the alloy  $x=0.50$  using  $\text{Cu K}\alpha$  radiation. The first maximum is seen to be  $14^\circ$  wide full width at half maximum (FWHM) as compared to a FWHM of  $5^\circ$ – $7^\circ$  for most metallic glasses.<sup>8</sup> Another interesting observation is the intensity of the second maximum. Unlike most metallic glasses, and akin to the Rh-B-Si glasses,<sup>1</sup> the second maximum is almost as intense as the first.

Figure 2 shows the reduced interference functions  $i(K)=K[I(K)-1]$  for the three glasses with  $x=0.46$ , 0.48, and 0.52. In all three cases we note the unusual fact that the second peak is larger than the first. This was also noted for the alloy  $\text{Rh}_{60}\text{B}_{32}\text{Si}_8$ .<sup>1</sup> The similarity between the reduced interference functions for  $(\text{Ru}_{0.84}\text{Zr}_{0.16})_{54}\text{B}_{46}$  in the transmission and reflection geometries (Fig. 2) clearly precludes the possibility of an oriented microcrys-

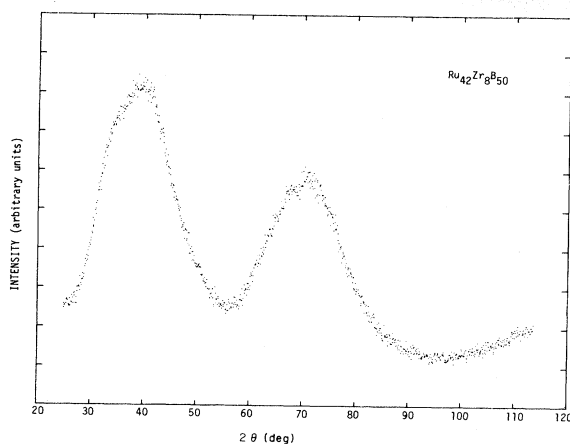


FIG. 1. X-ray-diffraction pattern for the alloy  $\text{Ru}_{42}\text{Zr}_8\text{B}_{50}$  obtained by using  $\text{Cu } K\alpha$  radiation.

talline structure.

The reduced radial distribution functions  $G(r)$  shown in Fig. 3 were obtained by using the relation<sup>4</sup>

$$G(r) = 4\pi r [\rho(r) - \rho_0] \approx \frac{2}{\pi} \int_0^{K_{\max}} K [I(K) - 1] U(K) \times \sin(Kr) dK .$$

Here,

$$U(K) = \frac{\sin(\pi K / K_{\max})}{\pi K / K_{\max}}$$

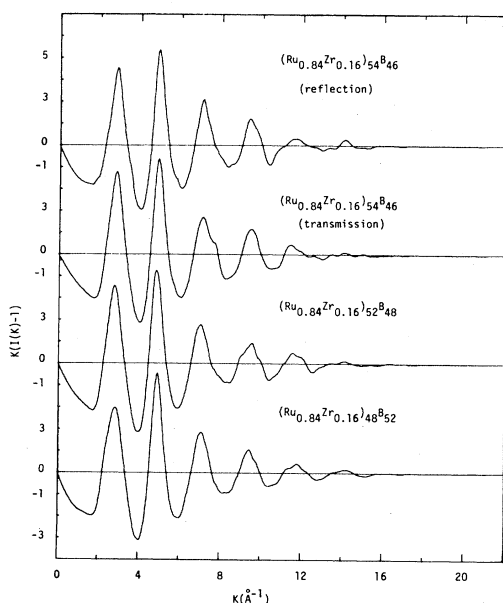


FIG. 2. Reduced interference functions  $i(K) = K[I(K) - 1]$  for the three alloys with  $x = 0.46, 0.48$ , and  $0.52$ . For  $x = 0.46$  the  $i(K)$  obtained in both the reflection and transmission geometries are shown.

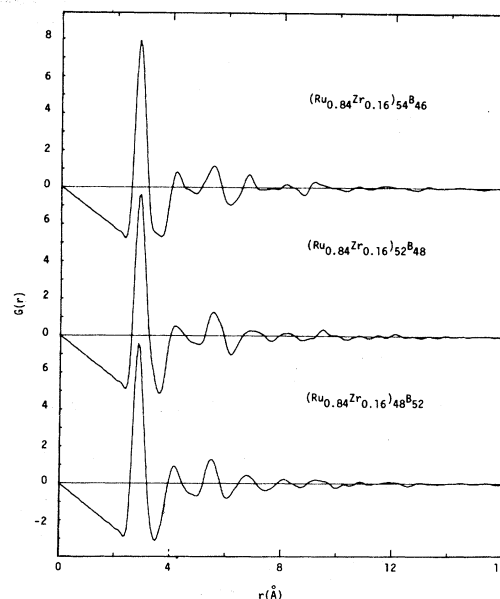


FIG. 3. Reduced RDF's  $G(r)$  for the three alloys with  $x = 0.46, 0.48$ , and  $0.52$ .

is the Lorch filter and is employed as a convergence factor. The implications of its use have been discussed in Ref. 9. The interference functions shown in Fig. 2 have been multiplied by  $U(K)$ , with  $K_{\max} = 17.0 \text{ \AA}^{-1}$ , which was the maximum  $K$  vector accessible with  $\text{Mo } K\alpha$  radiation.

If, instead of the  $G(r)$ , we define the radial distribution function (RDF) as  $\mathcal{F}_{\text{RDF}}(r) = 4\pi r^2 \rho(r)$ ; then information about the atomic coordination in the material can be obtained. The average radial dependence of the atomic density  $\rho(r)$  can be written as<sup>4</sup>

$$\rho(r) \approx \sum W_{ij} \rho_{ij}(r) / c_j ,$$

with

$$W_{ij} = c_i c_j Z_i Z_j / |\langle Z \rangle|^2 \text{ and } \sum W_{ij} = 1 .$$

Here  $c_i$  is the fractional atomic composition of constituent  $i$ ,  $Z_i$  is its atomic number, and  $\rho_{ij}(r)$  is the average atomic density of  $j$ -type atoms, a distance  $r$  from an average  $i$ -type atom. The angular brackets denote a compositional average. In the alloys under consideration,  $(\text{Ru}_{0.84}\text{Zr}_{0.16})_{1-x}\text{B}_x$ , the major contributions to the diffracted intensity and hence to the  $\rho(r)$ , are from Ru-Ru, Ru-Zr, and Ru-B pairs. Table I lists the weighting factors  $W_{ij}$  for the three compositions. We obtain a value for the weighted sums of the various atomic coordinations from

$$\eta = \int_0^{R_{\min}} 4\pi r^2 \rho(r) dr ,$$

where  $R_{\min}$  is the minimum in  $\rho(r)$ , immediately following the primary maximum.

The positions of the first four maxima in the  $G(r)$  shown in Fig. 3 are listed in Table II, along with the atomic densities and the coordination numbers, calculated as above.

Upon comparing these reduced RDF's with those ob-

TABLE I. List of the weighing factors,  $W_{ij}$ , for the three alloys.

$W_{ij}$	$(\text{Ru}_{0.84}\text{Zr}_{0.16})_{54}\text{B}_{46}$	$(\text{Ru}_{0.84}\text{Zr}_{0.16})_{52}\text{B}_{48}$	$(\text{Ru}_{0.84}\text{Zr}_{0.16})_{48}\text{B}_{52}$
Ru-Ru	0.60	0.59	0.57
Ru-Zr	0.21	0.21	0.20
Ru-B	0.14	0.15	0.17
Zr-Zr	0.02	0.02	0.02
Zr-B	0.02	0.03	0.03
B-B	0.01	0.01	0.01

tained for binary relaxed DRP models,<sup>4</sup> it is evident that there is a considerable difference in the predicted and observed peak positions. While, admittedly, we are comparing these alloys of high boron content to DRP models proposed for alloys with less than 25 at. % metalloid, it is not at all clear what similar algorithms would give for binary or ternary alloys with 50 at. % B. In view of that, this comparison is to emphasize the need for a radically different approach to the problem, rather than to criticize already existing, and in some cases successful, models. We therefore attempt to explain the structure in terms of trigonal prismatic packing (TPP), as proposed by Gaskell.<sup>5</sup>

In the compositionally related crystalline phases of most "traditional" transition-metal-metalloid glasses there is an almost universal occurrence of trigonal prismatic coordination. This packing of  $NM_6$  trigonal prisms is found in crystalline phases ranging over wide compositions: from  $\text{MoP}_2$ <sup>10</sup> to  $\text{Pd}_6\text{P}$ .<sup>11</sup> Gaskell has therefore suggested that this kind of coordination would also be expected to represent the "dominant motif" in the glass state.<sup>5</sup> Keeping this in mind, we first look for the crystalline phases of Ru-B that contain packings of trigonal prisms. While the structure of  $\text{RuB}$  has been proposed as cubic,<sup>12</sup> it has as yet not been studied in detail. However,  $\text{RuB}_2$  is known to form the  $\text{AlB}_2$  structure [Fig. 4(a)]. The unit cell of  $\text{AlB}_2$  is hexagonal, and there is one formula weight per unit cell. The metal atom is at the origin (0,0,0), and the B atoms are positioned at  $(\frac{1}{3}, \frac{2}{3}, \frac{1}{2})$  and  $(\frac{2}{3}, \frac{1}{3}, \frac{1}{2})$ . This results in alternate planar layers perpendicular to the  $c$  axis [Fig. 4(b)]. Each metal atom has six equidistant metal neighbors in its own plane and 12 equidistant B neighbors—six above and six below. In the particular case of  $\text{RuB}_2$ , the length of the  $a$  axis is determined primarily by the B-B distance since the Ru atom is relatively small. It turns out that the Ru-Ru distance in one plane,  $a$ , is 2.852 Å, while  $c$  equals 2.855 Å, resulting in a packing of trigonal prisms with almost square faces ( $c/a=1.001$ ). This now means that the nearest-neighbor Ru-Ru coordination is 8 while the nearest-neighbor Ru-B coordination remains 12.

The interesting aspect of this structure is that it immediately reproduces our nearest-neighbor distance of 2.86 Å (for  $x=0.48$ ). Further, the second-nearest neighbor

Ru-Ru distance in the  $\text{RuB}_2$  structure is 4.04 Å, while the same distance obtained from the  $G(r)$  is 4.14 Å, again in good agreement. It should be noted that the  $\sqrt{2}$  distance, which is not found in the DRP structure (and the absence of which is used to argue that octahedral coordination does not exist in DRP models<sup>4</sup>), is indeed present here.

As it stands, there are two problems with the  $\text{RuB}_2$  structural unit: It suggests a much higher B content than is actually present in our alloys, and it provides a third-nearest-neighbor Ru-Ru distance of  $\sqrt{3}R_1$ . This is the distance between two Ru atoms which form the vertices, in the same plane, of two trigonal prisms sharing a square face [distance  $AB$  in Fig. 4(a)]. No maximum is present at this distance in the  $G(r)$  obtained experimentally.

The first rule, then, for the packing of trigonal prisms would be that they do not share square faces. Instead, the short-range packing would either be in the form of corrugated chains as found in the  $\text{MoP}_2$  structure,<sup>10</sup> or the square faces would be capped [Fig. 4(c)] and two trigonal prisms would share only an edge common to their triangular faces, as in the  $\text{Fe}_3\text{C}$  structure.<sup>5</sup> The former structure provides the third-nearest-neighbor Ru-Ru distance of  $2R_1$ . Yet another mode of packing could be that capped trigonal prisms, like one of the canonical holes of a DRP structure,<sup>4</sup> are stacked around and on top of each other [Fig. 4(e)]. The packing would then be in terms of such capped trigonal prisms with a B atom within, and tetrahedra formed between the capping atoms of two layers and the two atoms of the triangular edge on the plane in between them [ $ABCD$  in Fig. 4(e)]. The packing in the plane of the capping atoms would be distorted since the undistorted vertex angle of the half-octahedron is about 75°, and this would require 4.8 half-octahedra to fill space. With some distortion, five half-octahedra could be fitted sharing the vertex atom, but the fivefold symmetry of the cluster would still prevent the complete filling of space. This is just what we require for the frustration of the alloy into a glassy state. The distortion would also result in increasing the  $AB$  distance in Fig. 4(e) to 2.82 Å, which is almost equal to  $R_1$ . This structure would have a significant number of well-defined third-nearest neighbors at  $2R_1$ , and that would result in a well-defined peak in the  $G(r)$  at

TABLE II. Positions of the first four maxima in the  $G(r)$  shown in Fig. 3 listed along with the atomic densities and coordination numbers for the three alloys.

Alloy	$R_1$ (Å)	$R_2/R_1$	$R_3/R_1$	$R_4/R_1$	$\eta$	$\rho_0$ (atoms/Å <sup>3</sup> )
$(\text{Ru}_{0.84}\text{Zr}_{0.16})_{54}\text{B}_{46}$	2.83	1.47	1.94	2.39	16.6	0.09223
$(\text{Ru}_{0.84}\text{Zr}_{0.16})_{52}\text{B}_{48}$	2.86	1.45	1.92	2.41	17.2	0.09483
$(\text{Ru}_{0.84}\text{Zr}_{0.16})_{48}\text{B}_{52}$	2.84	1.46	1.92	2.38	15.9	0.09676

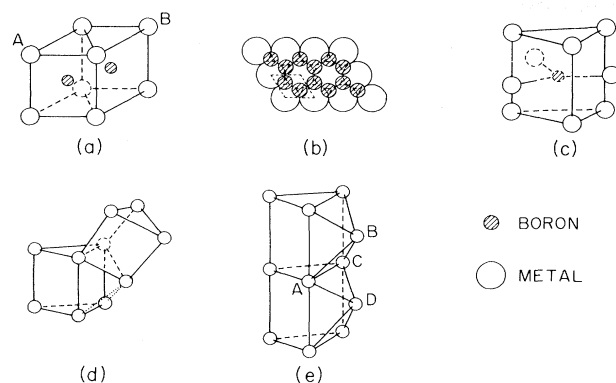


FIG. 4. (a) Unit cell of  $\text{AlB}_2$ , (b) Planar layers formed in the  $\text{AlB}_2$  structure, (c) Capped trigonal prism, (d)  $\text{Fe}_3\text{C}$  structure, and (e) TPP suggested for the  $(\text{Ru}_{0.84}\text{Zr}_{0.16})_{1-x}\text{B}_x$  glasses. In (d) and (e) only one capping atom is shown.

that distance rather than just a shoulder. This is indeed what is observed (Fig. 3). If only about half the capped trigonal prisms have a B atom within them, then the structure would collapse slightly, resulting in further disorder. It would also result in the correct metal-to-metalloid ratio for our alloys.

The role of the Zr atom is more difficult to quantify. It is expected that the presence of the Zr atoms enhances the disorder of the system. This would explain the lower limit in the concentration range for Zr as mentioned earlier. As the Zr concentration is increased, it is possible that the Zr atom's greater affinity for B causes it to define its own environment rather than merely play the role of increasing disorder, resulting in a loss of the glassy state. The inability of titanium to replace Zr may be because of its considerably smaller size.

No systematic compositional dependence of the structure is evident, except that the second and third peaks are better resolved in the  $G(r)$  as we increase the B content of the alloy. This would mean that the third-nearest neighbors are better defined for higher B concentrations. This is not unexpected in view of the findings of Boudreaux *et al.*, that the number of trigonal prisms observed in simulations of Fe-B glasses increased with B content.<sup>13</sup> While their analysis is restricted to B contents of up to 25 at. %, it may not be entirely unreasonable to extrapolate to higher B concentrations. With larger numbers of trigonal prisms we would expect more clusters of TPP, resulting in a well-defined third-nearest-neighbor distance of  $2R_1$ .

The coordination number obtained in all three cases is approximately the same, and this is indeed what we expect since we have proposed that the local coordination in all three glasses is the same. To within the error of  $\pm 1$  in the

composite coordination number, there is no compositional dependence of  $\eta$ .

These metallic glasses have the highest atomic densities reported to date.<sup>14</sup> Further, the density is seen to increase with B content. This is reasonable since the B atoms would fill the available trigonal prisms without a significant increase in volume. Even though the atomic densities are high, the packing fraction defined by

$$P_F = \frac{4}{3} \pi \frac{\langle R_g^3 \rangle}{\langle V \rangle},$$

where  $R_g$  are the Goldschmidt radii<sup>15</sup> and the angular brackets denote compositional averages, is typical of that of most metallic glasses (for  $x=0.52$ ,  $P_F=0.625$ ). Here we have used the Goldschmidt radius for boron in order to obtain an upper limit for packing fraction. This typical value for  $P_F$  obtained in spite of the large value for the boron radius, would lead us to believe that the reason for the high atomic density is the presence of a large fraction of small metalloid atoms rather than a denser packing of the atoms.

## CONCLUSIONS

X-ray-diffraction studies of  $(\text{Ru}_{0.84}\text{Zr}_{0.16})_{1-x}\text{B}_x$  metallic glasses in the range  $0.46 \leq x \leq 0.52$  indicate that available DRP models are inadequate to explain the structure of these glasses. Instead, they have a well-defined trigonal prismatic short-range order, and the clustering of such trigonal prisms can be used to explain the main features of the experimentally obtained  $G(r)$ . These glasses have very high atomic densities which result due to the presence of an unusually large fraction of small metalloid atoms. As a follow up of this work, we propose to use small-angle x-ray scattering in an attempt to determine the size of the trigonal prismatic clusters, and carry out crystallization studies which would help confirm the proposed short-range order. Also, extended x-ray-absorption fine structure (EXAFS) on the Zr site will be carried out and will help shed some light on the environment of the Zr atoms and their role in the formation of the amorphous phase.

## ACKNOWLEDGMENTS

We would like to thank Professor Pol Duwez, who, with his inimitable humor and good-natured encouragement, has been an inspiration to us all in our work. We would also like to thank Vladimir Matijasevic for his help in developing the computer programs. We gratefully acknowledge the financial support provided by the U.S. Department of Energy under Project agreement No. DE-AT03-81ER-10870 and Contract No. DE-AM03-76-SF-00767.

<sup>1</sup>A. Williams, M. Mehra, and W. L. Johnson, *J. Phys. F* **12**, 1861 (1982).

<sup>2</sup>G. S. Chadha, N. Cowlam, H. A. Davies, and I. W. Donald, *J. Non-Cryst. Solids* **44**, 265 (1981).

<sup>3</sup>A. Inoue, A. Kitamura, and T. Masumoto, *Trans. Jpn. Inst. Met.* **20**, 404 (1979).

<sup>4</sup>See, e.g., G. S. Cargill III, *Solid State Phys.* **30**, 227 (1975).

<sup>5</sup>P. H. Gaskell, *J. Non-Cryst. Solids* **32**, 207 (1979).

<sup>6</sup>P. Pietrokowsky, *Rev. Sci. Instrum.* **34**, 445 (1963).

<sup>7</sup>C. N. J. Wagner, *Adv. X-Ray Anal.* **12**, 50 (1969).

<sup>8</sup>See, e.g., A. K. Sinha and P. Duwez, *J. Phys. Chem. Solids* **32**, 267 (1971).

<sup>9</sup>E. Lorch, J. Phys. C 2, 229 (1969).

<sup>10</sup>S. Rundqvist, Ark. Kemi 20, 67 (1963).

<sup>11</sup>Y. Andersson, V. Kaewchausilp, M. Soto, and S. Rundqvist, Acta Chem. Scand. 28, 297 (1974).

<sup>12</sup>C. J. Kempter and R. J. Fries, J. Chem. Phys. 34, 1994 (1961).

<sup>13</sup>D. S. Boudreaux and H. J. Frost, Phys. Rev. B 23, 1506 (1981).

<sup>14</sup>See, e.g., W. L. Johnson and A. R. Williams, Phys. Rev. B 20, 1640 (1979).

<sup>15</sup>Sargent-Welch tables, Cat. No. S-18806, Sargent-Welch Scientific Co.